

# Relationship between the ionospheric conductance, field aligned current, and magnetopause geometry: Global MHD simulations

V.G. Merkin<sup>a,\*</sup>, A.S. Sharma<sup>b</sup>, K. Papadopoulos<sup>b</sup>, G. Milikh<sup>b</sup>, J. Lyon<sup>c</sup>, C. Goodrich<sup>a</sup>

<sup>a</sup>Center for Space Physics, Boston University, Boston, Massachusetts, USA

<sup>b</sup>Department of Astronomy, University of Maryland, College Park, Maryland, USA

<sup>c</sup>Department of Physics and Astronomy, Dartmouth College, Hanover, New Hampshire, USA

Received 21 April 2004; received in revised form 16 February 2005; accepted 6 April 2005

Available online 24 May 2005

## Abstract

The role of the ionospheric conductance in the solar wind–magnetosphere coupling is studied using global MHD simulations. The simulations with varying conductance and a constant solar wind input show that the field-aligned currents, whose magnitude depends on the ionospheric conductance, affect the size of the magnetopause at the flanks by increasing the local magnetic pressure and thus altering the surface equilibrium at the magnetopause. A current system that generates the magnetic stresses required to account for the location and geometrical structure of the magnetosphere observed in the simulations is proposed.

© 2005 Elsevier Ltd. All rights reserved.

**Keywords:** Field aligned currents; Magnetopause geometry; Ionospheric conductance; Cross polar cap potential

## 1. Introduction

The magnetopause is usually defined as a surface across which the total pressure balance is maintained: the magnetic field pressure due to the earth's dipole balances the solar wind dynamic pressure on the outside. The contributions from thermal plasma pressure and solar wind magnetic field pressure are usually small and can be neglected. Further, the solar wind flow velocity is tangential to the magnetopause at all points (in the absence of magnetic reconnection). As a result the magnetopause is often considered as an obstacle in the way of the solar wind flow. Many aspects of the solar wind–magnetosphere–ionosphere (SW–M–I) interaction have been studied based on a supersonic hydrodynamic flow of the solar wind past an obstacle (Petrinec and Russell, 1997, and references therein). The size and shape of the magnetopause are determined by the fluid

properties of the solar wind and by the conditions of the internal magnetic field and plasma, which are affected by the ionosphere. Among the physical variables of the ionosphere its conductance is a key variable due to its direct effect on the evolution of the currents and consequently the magnetic field.

Merkin et al. (2003) have suggested, based on global MHD simulations, a mechanism for the ionospheric feedback on the reconnection potential leading to the saturation of the latter and consequently of the transpolar potential. This mechanism involves a self-consistent reconfiguration of the SW–M–I system in response to changes in the ionospheric conductance. An increase in the ionospheric conductance leads to the widening of the magnetopause at the flanks through the field aligned currents (FACs), creating an additional magnetic pressure inside the magnetopause and thus changing the pressure balance conditions at its surface (Merkin et al., 2003). As a result the flow in the magnetosheath can be significantly modified while the solar wind conditions upstream of the bow shock remain the same. This in turn can result in changes in

\*Corresponding author. Tel.: +1 617 358 3441.

E-mail address: [vgm@bu.edu](mailto:vgm@bu.edu) (V.G. Merkin).

the behavior of the SW–M–I system leading to the reduction of the reconnection and transpolar potentials.

In this paper, the results of a detailed study of the effect of the ionospheric conductance on the inter-relationship between the field-aligned currents and the location of the magnetopause are presented. These results complement the physical mechanism of transpolar potential saturation presented in Merkine et al. (2003).

## 2. MHD simulations of the solar wind–magnetosphere coupling for varying ionospheric conductance

A set of global MHD simulations using the Lyon–Fedder–Mobarry (LFM) code (Fedder and Lyon, 1995) was conducted for constant solar wind input conditions and variable Pedersen conductance in the ionosphere. The flow speed of  $v_x = -400$  km/s, corresponding to the purely anti-sunward solar wind, southward magnetic field  $B_z = -40$  nT, and  $n = 30$  cm<sup>-3</sup> were used. The Pedersen conductance,  $\Sigma_P$ , was taken equal to 1, 2.5, 5, 10, 15 and 20 S, respectively, and in each case the code was run for 5 h after the IMF southward turning so that a steady state was reached (Slinker et al., 1995).

Fig. 1a shows the dependence of the cross polar cap potential,  $\Phi_{PC}$ , and of the integrated FAC in the ionosphere, averaged over 40 min during the steady state, on  $\Sigma_P$ . As the conductance changes from 1 to 20 S,  $\Phi_{PC}$  drops by a factor of approximately 6, from 1200 to 200 kV. Correspondingly, the FAC grows from about 5 to 10 MA. The current and the voltage are found to be related as  $I = \xi \Sigma_P \Phi_{PC}$ , where  $\xi$  is a coefficient dependent on the geometry of the currents in the ionosphere with a value between 3 and 4. This is consistent with the results of Siscoe et al. (2002b).

The dependence of the size of the magnetopause on the conductance  $\Sigma_P$  is demonstrated by Fig. 1b. Here, the size of the magnetopause is defined as the distance along the GSM  $y$ -axis between the center of the earth and the magnetopause, determined by the location of the mass density jump. Figs. 1a and b show the tendency of the magnetopause to widen when the ionospheric conductance increases while the solar wind remains constant (Merkine et al., 2003) and also this tendency is robust over a wide range of values of  $\Sigma_P$ . An important feature of Figs. 1a and b is the presence of clear saturation effects on  $\Phi_{PC}$  and  $I$  as well as the size of the magnetopause. The relationship between the polar cap potential and the currents will be discussed in Section 5.

## 3. Pressure balance and the magnetopause size

The magnetopause equilibrium requires a balance of the total pressure across the discontinuity, which can be

written as follows (Spreiter et al., 1966):

$$\frac{(2fB_{\text{dip}})^2}{8\pi} = \kappa \rho v_{\text{sw}}^2 \cos^2 \theta, \quad (1)$$

where the variables are the dipole magnetic field inside the magnetopause  $B_{\text{dip}}$ , the solar wind plasma density  $\rho$ , the solar wind velocity  $v_{\text{sw}}$ , and the angle between the magnetopause normal and the sun–earth line or the flaring angle  $\theta$ . On the right-hand side of Eq. (1) the magnetosheath pressure at a point on the magnetopause is expressed in terms of the solar wind ram pressure upstream of the bow shock and the flaring angle at that point (Newtonian approximation). Eq. (1) assumes that the compressed dipole magnetic field has a value twice its uncompressed value and the coefficient  $f$  describes deviation from this assumption. The coefficient  $\kappa$  represents the ratio of the stagnation point static pressure to the solar wind dynamic pressure upstream of the bow shock as well as the uncertainty due to the Newtonian approximation. On the symmetry axis of the flow (where  $\theta = 0$ ) the coefficient  $\kappa$  can be obtained analytically by considering the process to be purely hydrodynamic (Landau and Lifshitz, 1959). For flow Mach numbers greater than 2 (normally the Mach number of the solar wind flow is much higher)  $\kappa$  is less than 1 and converges steeply to the value of 0.88 with increasing Mach number. In general,  $\kappa$  is in the range from 0.67 to 1.0 and  $f$  from 1.0 to 1.5 (Sibeck et al., 1991).

The simulations described above show that an increase in the ionospheric conductance results in additional pressure inside of the magnetopause, since for the same solar wind dynamic pressure upstream of the bow shock the magnetopause moves farther out from the earth (at least at the flanks). To identify the sources of additional pressure required to satisfy the total pressure balance, the size of the magnetopause and the magnetopause subsolar point distance, computed readily in the simulations, are first determined and then the pressure balance equation is recast in terms of these geometrical characteristics. We start by describing the magnetopause as a general conic of revolution

$$r = \frac{\kappa}{1 + \varepsilon \cos \phi}, \quad (2)$$

where  $r$  is the distance from the focus (center of the earth) to a particular point on the surface,  $\phi$  is the angle from the sun–earth line to the point on the surface,  $\varepsilon$  is the eccentricity, which governs the shape of the magnetopause, and  $\kappa$  is the distance from the focus to the surface for  $\phi = 90^\circ$ , i.e. the size of the magnetopause as defined above.

To derive a relationship between  $\kappa$  and  $\cos \theta$ , we note that the equation for the normal to the conic of

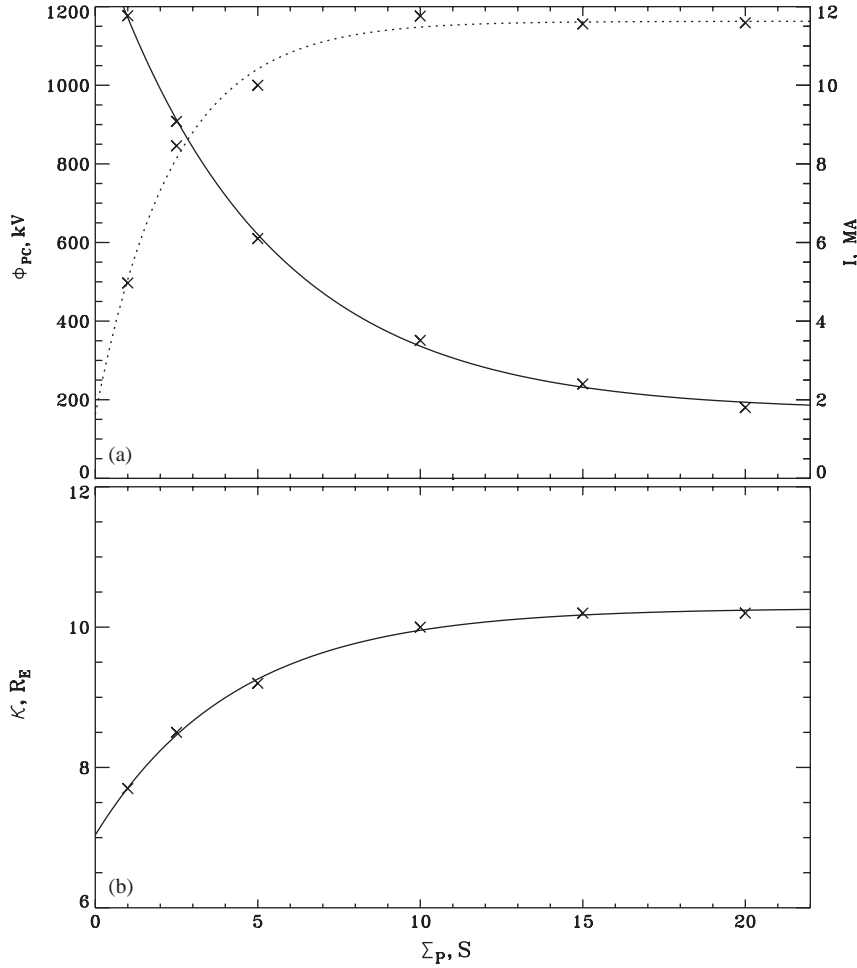


Fig. 1. The dependence on the ionospheric Pedersen conductance: (a) of the cross polar cap potential (solid line) and the ionospheric field aligned current (dashed line); (b) of the magnetopause size,  $\kappa$ . The lines are fits to the simulation data.

revolution at the point  $\phi = 90^\circ$  is

$$\vec{n} = \frac{1}{\sqrt{1 + \varepsilon^2}} \begin{pmatrix} \varepsilon \\ 1 \end{pmatrix}, \quad (3)$$

where  $\vec{n}$  is a two-dimensional unit vector lying in a plane containing the symmetry axis of the conic. Consequently,

$$\cos \theta = \frac{\varepsilon}{\sqrt{1 + \varepsilon^2}}. \quad (4)$$

The magnetopause subsolar point distance is determined from Eq. (2) when  $\phi = 0$

$$\frac{\kappa}{1 + \varepsilon} = D. \quad (5)$$

Finally, on expressing  $\varepsilon$  in terms of  $\kappa$  and  $D$ , Eq. (4) becomes

$$\cos \theta = \frac{\frac{\kappa}{D} - 1}{\sqrt{1 + \left(\frac{\kappa}{D} - 1\right)^2}}. \quad (6)$$

Eq. (6) allows one to express the solar wind dynamic pressure at the flanks of the magnetopause on the right-hand side of Eq. (1) in terms of distances easily determined in the simulations.

#### 4. Effect of field aligned currents on the magnetopause size

The field aligned currents provide a physical connection between the ionosphere and the magnetopause, and produce a magnetic field. This magnetic field modifies the total pressure inside the magnetopause and thus changes the location of the surface across which pressure balance is maintained. The idea that the FACs can significantly change the structure of the magnetic field inside the magnetopause was discussed earlier. Hill and Rassbach (1975) and Maltsev and Lyatsky (1975) independently proposed a model linking the erosion of the magnetopause during periods of the southward IMF to the distortion of the dipole magnetic field at the

subsolar point by the additional magnetic field produced by the FAC loop. Further, the Hill model of the cross polar cap potential saturation (Hill et al., 1976; Siscoe et al., 2002b) is based on the recognition that the dipole magnetic field at the subsolar point is reduced significantly by the magnetic field due to the FAC. Similar considerations are used here, although we analyze the magnetopause location at the flanks, rather than at the subsolar point. The role of the FACs in the magnetopause pressure balance was also noted by Siscoe et al. (2002a).

The effect of the magnetospheric erosion may be quite important in context of the present paper. The magnetopause flattening, whether it be due to the widening at the flanks or due to the erosion, leads to the broadening of the magnetosheath which has significant effects on the reconnection and transpolar potentials (Merkine et al., 2003). It should be noted that in addition to the conductance dependent erosion effect due to the field aligned currents (Hill et al., 1976; Maltsev and Lyatsky, 1975) there exists a “zero offset” effect: the subsolar magnetopause distance inferred from the simulations for the given solar wind conditions (see Section 2) is  $\sim 5R_E$  while simple pressure balance Eq. (1) yields  $\sim 8.3R_E$ . This 40% difference is due to the combined effects of the field aligned currents and inaccuracies in Eq. (1). The computed magnetopause subsolar distance changes by approximately  $0.5\text{--}1R_E$  from  $5.5\text{--}6$  to  $5R_E$  as  $\Sigma_P$  varies from 1 to 20 S adding a variance of 10–20% to the above effect. On the other hand, the analysis of Fig. 1b yields a  $\sim 25\%$  effect of the

changing ionospheric conductance on the flank magnetopause distance:  $\kappa$  changes from 7.5 to  $10R_E$ . Therefore, the magnetospheric erosion is complementary to the effect discussed here and its role in the saturation of the cross polar cap potential should be studied in detail. However, the main focus of this paper is the effect of the FAC on the magnetopause location at the flanks and therefore we shall not consider the influence of the subsolar magnetopause erosion here.

We start by considering the FAC in the MHD simulations. The  $z$ -component of the current density for the simulation with  $\Sigma_P = 10\text{ S}$  is shown in Fig. 2 and the current flow-path can be represented schematically by the dashed line. The magnetic fields produced by the southern (lower) and the northern (upper) current loops cancel each other on the  $y$ -axis in the equatorial plane. However, for the  $z = 1R_E$  plane, the current loop shown in Fig. 2 drives a rather strong positive  $x$ -directed (pointing out of the plane) magnetic field at the flank (for positive  $y$  and  $z$  coordinates) just between the downward and upward current branches. Fig. 3 shows the profiles of the magnetic field  $x$ -component along the  $y$ -axis in the  $z = 1$  plane for the cases with  $\Sigma_P = 2.5$  and 10 S. As a result of the additional magnetic field pressure inside the magnetopause the flaring angle increases and the location of the magnetopause changes to maintain a new pressure balance for the given solar wind conditions.

In Fig. 3 one can see a noticeable negative  $x$ -component of the magnetic field closer to the earth. It is a signature of the sunward plasma convection

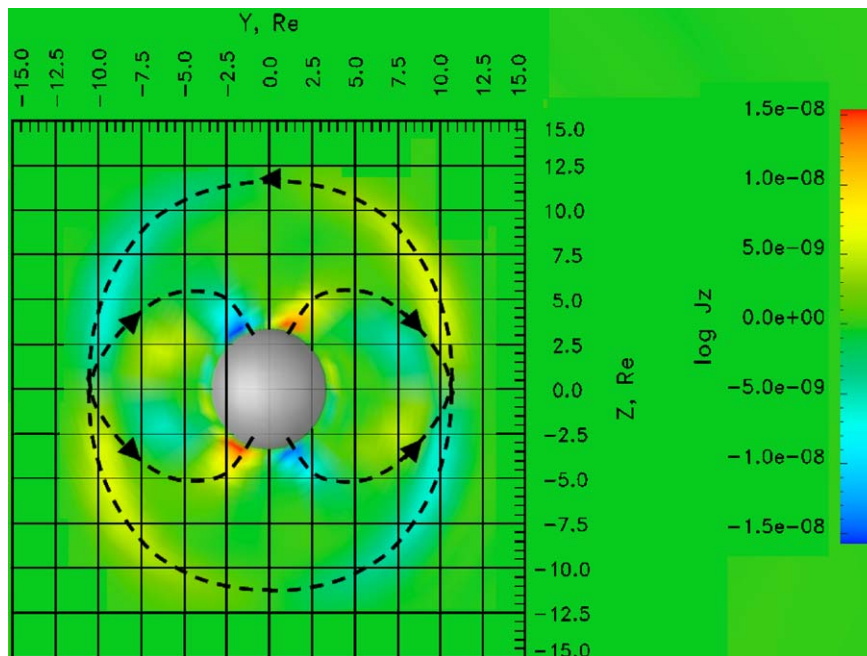


Fig. 2. A sketch of the current loop in the terminator plane. The background shows the  $z$ -component of the current density in the terminator plane for the simulation with  $\Sigma_P = 10\text{ S}$ .

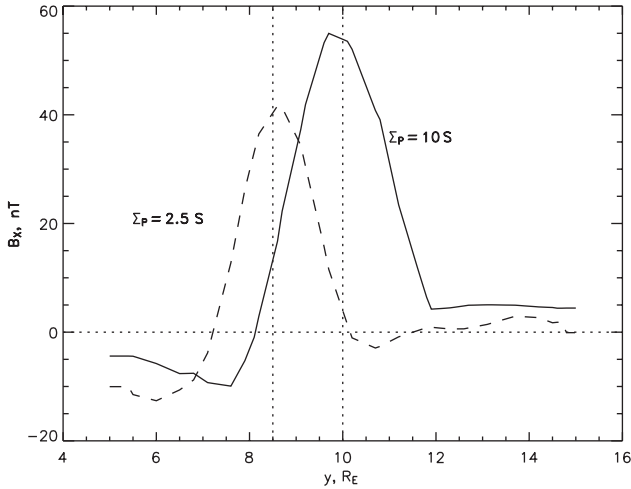


Fig. 3. Profiles of  $B_x$  along the GSM  $y$ -axis in the  $z = 1R_E$  plane for shown values of the conductance. The vertical dashed lines denote the location of the magnetopause as defined by the density jump.

in the inner magnetosphere common to global MHD simulations of the magnetosphere under steady southward IMF driving (Mobarry et al., 1996; Ridley et al., 2001). The sunward plasma convection leads to the sunward dragging of the otherwise dipolar magnetic field lines in the inner magnetosphere region. This results in a small negative  $x$ -component of the magnetic field, which is about 10–15% of the background dipole magnetic field for the  $\Sigma_P = 10$  S case shown in Fig. 3.

In order to verify that the FAC (and therefore indirectly, ionospheric conductance) is responsible for the displacement of the magnetopause at the flanks we consider below two cases,  $\Sigma_P = 2.5$  and  $= 10$  S in detail. We shall first calculate the displacement of the magnetopause, quantified by the change in the flaring angle  $\Delta(\cos^2 \theta)$ , given the increase in the internal magnetic pressure using Eq. (1). This will then be compared with the displacement inferred directly from determination of the magnetopause geometric characteristics using Eq. (6). Agreement of the two estimates would confirm the role of the FAC in the control of the magnetopause.

Including the FAC and neglecting the internal plasma pressure and the perturbations of  $B_y$  and  $B_z$  compared to those of  $B_x$ , the magnetic pressure inside the magnetopause becomes

$$P = \frac{(2fB_{\text{dip}})^2}{8\pi} + \frac{B_x^2}{8\pi}. \quad (7)$$

Assuming that the change in the ionospheric conductance is responsible for the widening of the magnetosphere at the flanks, while the compressed dipole field and the coefficients  $\kappa$  and  $f$  remain the same, we obtain from Eq. (1) the changes across the

magnetopause

$$\frac{\Delta\left(\frac{B_x^2}{8\pi}\right)}{\rho v_{\text{sw}}^2} = \kappa \Delta(\cos^2 \theta), \quad (8)$$

where the dipole part of the field has been canceled.

Comparing the magnitudes of the field for the selected cases ( $\Sigma_P = 2.5$  and  $10$  S) we can estimate the variation in the flaring angle produced by the corresponding change of the magnetic pressure inside the magnetopause. The computed  $x$ -component of the magnetic field is found to be approximately 40 and 55 nT (see Fig. 3), respectively, and assuming  $\kappa \sim 1$  Eq. (8) yields

$$\Delta(\cos^2 \theta) \simeq 8 \times 10^{-2}. \quad (9)$$

This equation gives an estimate of the change in the size of the magnetopause following the increase in the strength of the FAC. On the other hand, substitution of the geometric characteristics of the magnetopause computed in the simulations ( $\kappa \simeq 8.5$  and  $10R_E$  for  $\Sigma_P = 2.5$  and  $10$  S, respectively, and  $D \simeq 5R_E$ ) into Eq. (6) yields  $\Delta(\cos^2 \theta) \simeq 1.7 \times 10^{-1}$ , which, considering the crudeness of the estimate, is in a good agreement with Eq. (9). This result confirms that the displacement of the magnetopause is due to the additional magnetic field driven by the FAC.

To further verify this picture we consider the pressure balance at the flanks of the magnetopause in a number of simulations. A straightforward way of doing this is to check the dependence of the FAC on the pressure just outside the magnetopause. This dependence can be examined in the  $(I^2, P)$  space, where  $I$  is the magnitude of the ionospheric integrated FAC and  $P$  is the total pressure  $p + B^2/8\pi$  just outside of the magnetopause at its flanks. Since the additional magnetic field produced by the current  $I$  is proportional to its magnitude the relationship between these two quantities is expected to be linear. However, computing the physical quantities at the surface of the magnetopause is complicated in the MHD code and we will utilize the results of Section 3, i.e. use the Newtonian approximation for the total pressure outside of the magnetopause and express it in terms of the easily determined distances.

Using Eq. (6), we recast the total pressure from outside the magnetopause in terms of the size  $\kappa$  and the subsolar point distance  $D$ . Then we calculate  $\cos \theta$  for each case since we are able to determine  $\kappa$  and  $D$ , and estimate the accuracy of this procedure. According to Eqs. (1) and (7) the dependence of  $\cos^2 \theta$  on the square of the ionospheric FAC is expected to be linear. In Fig. 4 we present this dependence along with the error bars calculated by assuming that the accuracy in the computation of  $\kappa$  and  $D$  is equal to  $\sim 0.3R_E$ , the local code resolution. This figure clearly indicates the expected linear dependence. Note that Fig. 4 demonstrates the results of the

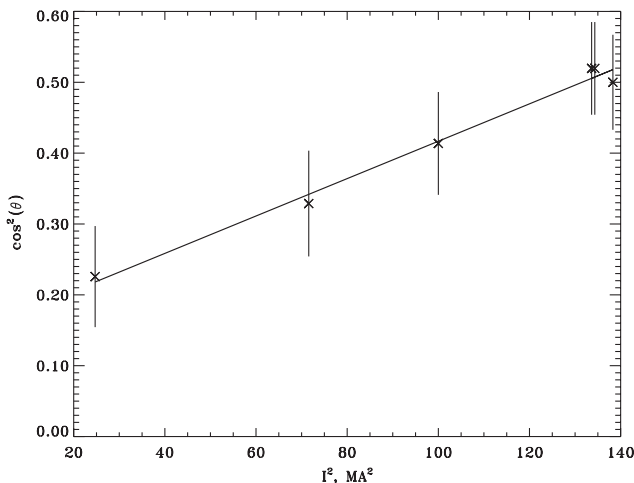


Fig. 4. The dependence of the squared cosine of the flaring angle on the squared magnitude of the ionospheric integrated current.

simulations, in which only the ionospheric conductance was varied while the solar wind conditions remained constant. This result confirms how the ionospheric conductance controls the size of the magnetopause: by regulating the strength of the FAC it influences the location of the magnetopause surface.

## 5. Discussion and conclusions

A series of global MHD simulations was performed using the LFM code to study the effect of the ionospheric conductance on the geometry of the magnetopause. It is found that the ionospheric conductance controls the size of the magnetopause at the flanks through the ionospheric FAC flowing in and out of the ionosphere. The current system creates an additional magnetic pressure inside the magnetopause that changes the pressure balance at its surface. Thus, for constant solar wind input, a change in the ionospheric conditions leads to a corresponding change in the geometry of the magnetopause. The dependence of the magnetopause size on the strength of the ionospheric FAC, obtained from the code, is shown to be consistent with the analytic results based on pressure balance considerations.

The study presented in this paper describes the physics of one of the components underlying the effect of the ionospheric conductance on the transpolar potential reported by Merkine et al. (2003). Based on the mechanism of Merkine et al. (2003) a qualitative interpretation of the shape of the lines in Figs. 1a and b can be given. Consider a situation when the magnetosphere is driven by a steady solar wind at a given value of  $\Sigma_P$ . The applied cross magnetosphere (reconnection) potential drives a FAC of a certain magnitude. With an increase of  $\Sigma_P$  the FAC will tend to grow since the

driving potential has not changed. However, the growing current will push the magnetopause outward at the flanks and this will result in the magnetosheath broadening and the reduction of the reconnection potential as described in (Merkine et al., 2003). The reduced driving potential will, in turn, result in the weakening of the driven current. This explains the shape of the curves and, in particular, the saturation of the quantities in Figs. 1a and b, and emphasizes the strong relation between them. It should be noted that the effect of the magnetosphere erosion mentioned in Section 4 strengthens the effect discussed here since it similarly flattens the magnetopause and broadens the magnetosheath.

The mechanism of the ionospheric conductance control of the magnetopause presented here provides a means for the ionospheric conductance feedback on global properties of the SW–M–I system such as the transpolar potential. This mechanism complements the model of the transpolar potential saturation outlined in Merkine et al. (2003).

## Acknowledgements

This research was supported by NASA grants NAG513452 and NAG510882, and NSF grant ATM-0119196 and ATM-031829. We thank NCSA for computational resources used to complete the simulations.

## References

- Fedder, J.A., Lyon, J.G., 1995. The Earth's magnetosphere is  $165R_E$  long: self consistent currents, convection, magnetospheric structure, and processes for northward interplanetary magnetic field. *J. Geophys. Res.* 100, 3623.
- Hill, T.W., Rassbach, M.E., 1975. Interplanetary magnetic field direction and the configuration of the day side magnetopause. *J. Geophys. Res.* 80, 1–6.
- Hill, T.W., Dessler, A.J., Wolf, R.A., 1976. The role of ionospheric conductivity in the acceleration of magnetospheric particles. *Geophys. Res. Lett.* 3, 429–432.
- Landau, L.D., Lifshitz, E.M., 1959. *Fluid Mechanics*. Pergamon Press, New York.
- Maltsev, Y.P., Lyatsky, W.B., 1975. Field-aligned currents and erosion of the dayside magnetopause. *Planet. Space Sci.* 23, 1257–1260.
- Merkine, V.G., Papadopoulos, K., Milikh, G., Sharma, A.S., Shao, X., Lyon, J., Goodrich, C., 2003. Effects of the solar wind electric field and ionospheric conductance on the cross polar cap potential: results of global MHD modeling. *Geophys. Res. Lett.* 30 (23), 2180.
- Mobarry, C.M., Fedder, J.A., Lyon, J.G., 1996. Equatorial plasma convection from global simulations of the Earth's magnetosphere. *J. Geophys. Res.* 101, 7859–7874.
- Petrinec, S.M., Russell, C.T., 1997. Investigations of hydrodynamic and magnetohydrodynamic equations across the bow shock and along the outer edge of planetary obstacles. *Adv. Space Res.* 20, 743–746.

- Ridley, A.J., De Zeeuw, D.L., Gombosi, T.I., Powell, K.G., 2001. Using steady state MHD results to predict the global state of the magnetosphere-ionosphere system. *J. Geophys. Res.* 106, 30067–30076.
- Sibeck, D.G., Lopez, R.E., Roelof, E.C., 1991. Solar wind control of the magnetopause shape, location, and motion. *J. Geophys. Res.* 96, 5489–5495.
- Siscoe, G.L., Crooker, N.U., Siebert, K.D., 2002a. Transpolar potential saturation: roles of region 1 current system and solar wind ram pressure. *J. Geophys. Res.* 107, 1321.
- Siscoe, G.L., Erickson, G.M., Sonnerup, B.U.Ö., Maynard, N.C., Schoendorf, J.A., Siebert, K.D., Weimer, D.R., White, W.W., Wilson, G.R., 2002b. Hill model of transpolar potential saturation: comparisons with MHD simulations. *J. Geophys. Res.* 107.
- Slinker, S.P., Fedder, J.A., Lyon, J.G., 1995. Plasmoid formation and evolution in a numerical simulation of a substorm. *Geophys. Res. Lett.* 22, 859–862.
- Spreiter, J.R., Summers, A.L., Alksne, A.Y., 1966. Hydrodynamic flow around the magnetosphere. *Planet. Space Sci.* 14, 223–253.